**IF1 controls UCP1-dependent mitochondrial bioenergetics in brown adipocytes**

Henver S. Brunetta[1,2], Anna S. Jung[1,3], Annelise Francisco[4], Roger F. Castilho[4], Marcelo A. Mori[2,5,6], Alexander Bartelt[1,3,7]

[1]Institute for Cardiovascular Prevention (IPEK), Faculty of Medicine, Ludwig-Maximilians-University Munich, Germany
[2]Department of Biochemistry and Tissue Biology, University of Campinas, Campinas, Brazil
[3]Institute for Diabetes and Cancer (IDC), Helmholtz Center Munich, Neuherberg, Germany
[4]Department of Pathology, University of Campinas, Campinas, Brazil
[5]Obesity and Comorbidities Research Center (OCRC), University of Campinas, Campinas, SP, Brazil
[6]Experimental Medicine Research Cluster (EMRC), University of Campinas, Campinas, SP, Brazil
[7]German Center for Cardiovascular Research, Partner Site Munich Heart Alliance, Munich, Germany

**Short title:** IF1 in brown adipocyte mitochondrial bioenergetics

**Corresponding authors:**
Alexander Bartelt: alexander.bartelt@med.uni-muenchen.de
Marcelo A. Mori: morima@unicamp.br

**Abstract:**
In thermogenic adipocytes, uncoupling protein-1 (UCP1) is a key mediator of non-shivering thermogenesis (NST) by uncoupling the electron transport chain from $F_oF_1$-ATP synthase-mediated ATP production. While regulatory mechanisms of UCP1 are important for NST, it is unknown whether also the activity of ATP synthase is modulated during NST. Here, we show a critical role of Inhibitory Factor 1 (IF1), an inhibitor of ATP synthase, for brown adipocyte energy metabolism. In mice, IF1 protein content is diminished in brown adipose tissue of mice after 5 days of cold exposure. Additionally, the capacity of ATP synthase to generate mitochondrial membrane potential (MMP) through ATP hydrolysis (the so-called reverse mode) was higher in mitochondria isolated from cold-adapted mice compared to mice housed at room temperature. While silencing of IF1 in cultured brown adipocytes did not affect MMP, IF1 overexpression resulted in an inability of mitochondria to sustain MMP upon adrenergic stimulation. The effects of IF1 overexpression on MMP were blunted when UCP1 was silenced or when a mutant IF1, incapable of binding to ATP synthase, was used. In brown adipocytes, IF1 ablation was sufficient to increase mitochondrial lipid oxidation and the cellular dependency on glycolysis to produce ATP. Conversely, IF1 overexpression blunted mitochondrial respiration without causing energetic stress, leading to a quiescent-like phenotype in brown adipocytes. In conclusion, our data show that the cold-induced downregulation of IF1 facilitates the reverse mode of ATP synthase and enables proper bioenergetic adaptation of brown adipose tissue to effectively support NST.

**Graphical abstract:**

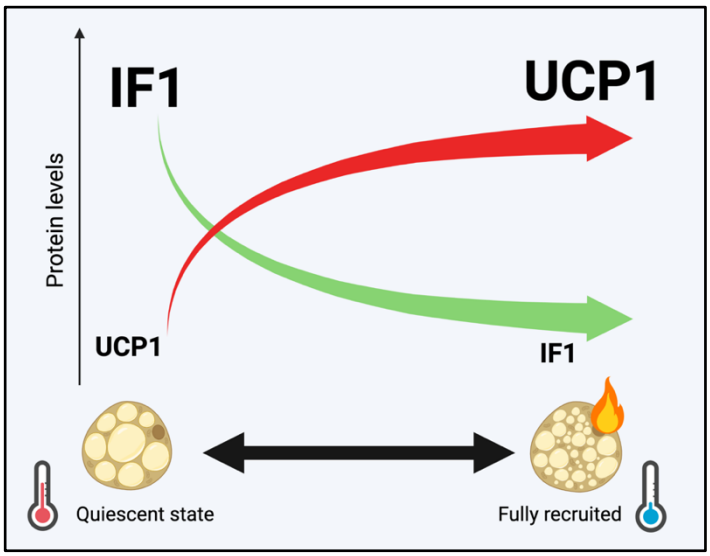


**Keywords:**
Adipocytes, thermogenesis, UCP1, ATP, mitochondria

**Abbreviations:**
*Atp5if1*: ATP synthase inhibitory factor subunit 1; BAT: brown adipose tissue; IF1: ATP synthase inhibitory factor 1; MMP: mitochondrial membrane potential; NST: non-shivering thermogenesis; PMF: protonmotive force; UCP1: uncoupling protein 1.

**Introduction:**
The primary function of brown adipose tissue (BAT) is non-shivering thermogenesis (NST)[1], which relies on the activation of uncoupling protein-1 (UCP1), a proton carrier that uncouples mitochondrial respiration from ATP synthesis. Activity of UCP1 is inhibited by purine nucleotides and stimulated by fatty acids, resulting in an increase in proton conductance across the inner mitochondrial membrane[2–5]. Thus, activation of UCP1 lowers mitochondrial membrane potential (MMP) and, consequently, increases the activity of the electron transport chain and mitochondrial oxygen consumption. As a result, cold exposure and adrenergic activation of BAT lead to increased whole-body oxygen consumption and energy expenditure[6,7]. Although the regulation of UCP1 is relatively well understood[1,2,8,9,10], very little is known regarding the mechanisms controlling $F_oF_1$-ATP synthase activity during NST. According to the chemiosmotic theory, the electrochemical gradient generated by the activity of the electron transport chain is coupled to ATP production by $F_oF_1$-ATP synthase[11]. $F_oF_1$-ATP synthase is a rotary motor protein catalyzing ATP synthesis from ADP and inorganic phosphate (Pi) by using the protonmotive force (PMF) across the inner mitochondrial membrane. Under specific conditions, $F_oF_1$-ATP synthase also functions as an ATPase (the so-called reverse mode), resulting in the formation of ADP plus Pi and leading to the reverse proton transport from the mitochondrial matrix into the intermembrane space[12], thus generating MMP. Therefore, when PMF is high, $F_o$ forcibly rotates $F_1$, resulting in ATP synthesis. Conversely, when PMF is low, $F_1$ reverses the rotation and hydrolyzes ATP. Given the vectorial dependence of ATP synthase on the MMP, it is intriguing to consider how ATP synthase would adapt following MMP modulation upon UCP1 activation in brown adipocytes.

Located in the mitochondrial matrix, ATP synthase inhibitory factor 1 (encoded by *Atp5if1,* hereafter called IF1), is activated when mitochondrial matrix pH is low, resulting in inhibition of ATP synthase[13–15]. IF1 inhibits the hydrolytic activity of ATP synthase when operating in the reverse mode[16]. This mechanism supposedly prevents cellular ATP depletion by mitochondria. However, it is now recognized that under certain conditions, such as low MMP or mitochondrial dysfunction, the reverse mode of ATP synthase is potentiated, generating MMP at the cost of mitochondrial ATP consumption[17–19]. Therefore, the role of IF1 controlling ATP synthase function seems to be more relevant to regulate cellular energy metabolism than previously assumed[18,36,37]. However, if IF1 plays a role in BAT energy metabolism during NST is unknown.

Here, we found that IF1 is downregulated in BAT of cold-adapted mice, allowing greater hydrolytic activity by ATP synthase. Using *in vitro* gain- and loss-of-function experiments in brown adipocytes, we determined that IF1 ablation is sufficient to elicit similar metabolic adaptations to those found in cold-adapted BAT. Conversely, IF1 overexpression blunts mitochondrial respiration, leading to a quiescent-like state and brown adipocyte deactivation. In summary, we establish IF1 downregulation as a key adaptative mechanism of NST to regulate brown adipocytes energy metabolism.

**Methods:**

*Mouse experiments*

All experiments were performed according to institutional guidelines and approved by the Animal Ethical Committee at the University of Campinas (5929-1/2021). Male C57BL/6J mice (12-15 weeks old) were randomly divided into room temperature (22 °C) or cold exposure (4 °C) groups. All animals were housed at the Institute of Biology animal facility on 12 h light:dark cycle with 24 h access to chow diet and water *ad libitum.*

*$F_oF_1$-ATP synthase hydrolytic activity*

$F_oF_1$-ATPase activity was measured in total BAT homogenates using a spectrophotometric method adapted from previous publication[20]. Briefly, 190 μL of reaction buffer containing 200 mM KCl, 20 mM HEPES, 10 mM $NaN_3$, 1 mM EGTA, 15 mM $MgCl_2$, and 10 mM phosphoenolpyruvate (pH 8) was added to a 96-well plate. Immediately before the reaction, 18 U/mL lactate dehydrogenase, 18 U/mL pyruvate kinase, 10 μL BAT homogenate, and 0.2 mM NADH were added to the well for a final volume of 0.2 mL. Assays were performed in triplicates at 37 °C and 340 nm wavelength. $F_oF_1$-ATPase activity was measured after the addition of 5 mM ATP. The slope of NADH disappearance after 5 min of reaction was used to calculate $F_oF_1$-ATPase and averaged among the triplicates. To assure $F_oF_1$-ATPase specificity, we used wells with the addition of oligomycin 1 μg/mL, which is an inhibitor of $F_o$-ATP synthase activity), or in the absence of ATP or $Mg^{2+}$, a cofactor necessary for $F_oF_1$-ATPase activity.

*Mitochondrial isolation*

Interscapular BAT mitochondria were isolated using differential centrifugation as previously described[21]. Tissues were harvested, minced in isolation buffer (100 mM sucrose, 100 mM KCl, 50 mM Tris-HCl, 1 mM $KH_2PO_4$, 0.1 mM EGTA, 0.2 % BSA, and 1 mM ATP; pH 7.4), weighed, and homogenized using a motorized Teflon pestle (800 rpm). Mitochondria were centrifuged at 800 g for 10 min, resuspended in 4 mL of isolation buffer, and immediately spun at 5000 g for 5 min. The pellet was repeatedly resuspended in respiration buffer (0.5 mM EGTA, 3 mM $MgCl_2{\cdot}6H_2O$, 60 mM K-lactobionate, 10 mM $KH_2PO_4$, 20 mM HEPES, 20 mM taurine, 110 mM sucrose, 1 g/L FFA-free BSA; pH 7.1) and pelleted at 10,000 g for 10 min. After protein quantification, 50 μg of mitochondria was used to determine mitochondrial membrane potential.

*ATP-supported mitochondrial membrane potential ($\Delta\Psi$)*

MMP was determined with 5 μM safranin-O dye added to the reaction medium as previously described[22,23]. Briefly, isolated mitochondria from BAT of room temperature or cold-exposed mice were incubated in the presence of antimycin A and GDP to inhibit flux through complex III and UCP1, respectively. After signal stabilization, ATP was added to the media to stimulate the reverse mode of ATP synthase and membrane potential generation. Oligomycin was used as a specificity control. Data are present as % of baseline signal obtained by safranin-O fluorescence.

*Cell culture*

Preadipocyte cells WT1 were cultured in growth medium DMEM GlutaMax (Thermo, cat. Num. 31966), 10 % v/v fetal bovine serum (FBS, Sigma), and 1 % v/v penicillin/streptomycin (PS, Sigma) and differentiated as previously described[24]. Briefly,

upon confluence, cells were differentiated from mature adipocytes by the addition of 1 μM rosiglitazone (Cayman), 1 nM T3 (Sigma), 850 nM human insulin (Sigma), 500 nM 3-isobutyl-1-methylxanthine (IBMX, Sigma), 1 mM dexamethasone (Sigma), and 125 nM indomethacin (Sigma) for 48 h, after which the medium was changed to a growth medium containing only rosiglitazone, T3, and insulin with this medium being renewed every 48 h. Primary brown adipocytes were obtained from interscapular brown adipose tissue of 6-8 weeks old C57BL/6N male mice. Tissues were minced and digested using collagenase 2 mg/mL at 37 °C under continuous agitation. Then, cells were filtered using 100 μm and 70 μm cell strainers and cultured in F12 media, 10 % v/v FBS (Sigma), and 1 % v/v PS (Sigma) until confluence. Upon confluence, cells were differentiated from mature adipocytes by the addition of 1 μM rosiglitazone (Cayman), 1 nM T3 (Sigma), 850 nM human insulin (Sigma), 500 nM IBMX (Sigma), and 1 mM dexamethasone (Sigma) for 48 h, after which the medium was changed to a growth medium containing only rosiglitazone, T3, and insulin with this medium being renewed every subsequent 48 h. Experiments in both cell lines were carried out on day 6 of the differentiation. NE treatment was carried out at 10 μM final concentration and treating the cells for 30 min. After that, western blots, membrane potential, or cellular ATP content were determined.

*IF1 gain- and loss-of-function experiments*

For the loss-of-function experiments, knockdown was achieved by using SMARTpool siRNA (Dharmacon). Transfection was performed on day 4 of differentiation using LipofectamineRNAiMAX transfection reagent (Thermo) and siRNA targeting *Atp5if1* and/or *Ucp1* at a concentration of 30 nM. SiScrambled was used as a control for silencing experiments. For the gain-of-function experiments, TOP10 bacteria were transformed by mixing 1 µL of Atp5if1_pcDNA3.1+/C-(K)-DYK plasmids and keeping them for 30 s at 42 °C. After that, bacteria were grown at 37 °C for 1.5 h and then streaked on an agar plate containing ampicillin (100 µg/mL) to be grown overnight also at 37 °C. The next day, a single colony was picked and inoculated into 5 mL LB medium with 100 µg/mL ampicillin. In the evening, 1 mL of the day culture was transferred into 400 mL LB medium with ampicillin for overnight culture. Maxiprep was performed according to the manufacturer's instructions (NucleoBond® Xtra Maxi Plus EF, Macherey-Nagel), and, after elution, DNA concentration was determined with Nanodrop and diluted to 1 µg/µl. Cells were transfected with the plasmid using TransIT-X2 diluted in Opti-MEM I Reduced-Serum Medium for 24 h according to the manufacturer's instructions. After transfection, cell media was replaced for another 24 h, and the experiments were performed. p-MXs-IF1(E55A) mutation was generated by David Sabatini's group and deposited at AddGene (cat. Number #85404)[18].

*Mitochondrial membrane potential (ΔΨ) determination*

To determine MMP, 20,000 differentiated WT1 cells were seeded in a well of a 96-well plate and transfected. 24 h after transfection, media was changed and kept for another 24 h. Then, the cells were treated with norepinephrine 1 μM for 30 min and stained with 20 nM TMRM for 30 min (Abcam, ab228569) according to the instructions of the fabricant. After that, cells were washed in imaging buffer and imaged using a Tecan plate reader at wavelength excitation/emission = 548/575 nm, respectively. Fluorescence was normalized relative to non-treated scrambled or empty vector cells in the presence or absence of norepinephrine.

*ATP levels and ATP/ADP ratio*

Cellular ATP levels were determined in differentiated WT1 cells by luminescence (Abcam, ab113849). Cells were transfected as previously described and acutely treated with 10 μM norepinephrine for 30 min. Thereafter, media was removed and cells were incubated in lysis buffer for 5 min under constant agitation (300 rpm). Then, ATP detection reaction buffer was added, and the samples were read in a Tecan plate reader according to the manual. Luminescence values were plotted against a standard curve provided by the manufacturer. To estimate ADP content, 100 μM dCTP (Sigma, cat. Num. 11934520001) and 5 U/mL nucleoside 5-diphosphate kinase (Sigma, cat. Num. N2635) were added, and luminescence was read again after 10 min[25].

*Cellular oxygen consumption and extracellular acidification rate*

Mitochondrial respiration was measured with Seahorse Cell Mito Stress Test (Agilent) with some adjustments. Briefly, primary brown adipocyte cells were cultured in a 24-well Seahorse plate on the fourth day of differentiation to be transfected. After transfection, culture medium was replaced with Seahorse medium (XF DMEM pH 7.4, 10 mM glucose, 1 mM pyruvate, 2 mM L-glutamine). To determine fatty acid-supported respiration, the medium was supplemented with 100 μM palmitate dissolved in 1 % w/v free fatty acid (FFA)-BSA. Cells were incubated for 60 min at 37 °C without $CO_2$ before being placed in the XFe24 instrument. 10 μM etomoxir was added in this step into the medium as indicated. In the assay, the cells were treated with NE (final concentration in the well was 1 μM), oligomycin (1 μM), FCCP (2 μM), and rotenone/antimycin A (0.5 μM). The reagents were mixed for 3 min, followed by 3 min of incubation, and 3 min of measurement. Afterwards, protein levels were measured for normalization using BCA assay (Thermo) according to the manual. To test the effects of fatty acids induced by lipolysis on mitochondrial uncoupling, mitochondrial respiration was also determined in the presence of Seahorse medium with 2% w/v FFA-BSA, as previously published[26].

*Glucose-dependent ATP production*

Glycolytic and oxidative ATP supply rates were calculated from cellular oxygen consumption and medium acidification as described[27], assuming that cellular energy metabolism was fueled exclusively by glucose. For that, we supplemented our media only with glucose. Sequential injections were made as follows: glucose (final concentration 10 mM), oligomycin (1 μM), and rotenone/antimycin A (0.5 μM). Glycolytic and oxidative phosphorylation ATP supply were calculated in the presence of glucose after subtracting oxygen consumption rate and extracellular acidification rate from oligomycin and rotenone/Antimycin A injection. After the experiment, total protein was measured for normalization using BCA assay (Thermo) according to the manual.

*Glycerol release*

Glycerol release was measured at baseline and upon adrenergic stimulation with norepinephrine as previously reported[24]. Briefly, we used Free Glycerol Reagent (Sigma, F6428) and Glycerol standard (Sigma, G7793) to measure free glycerol concentrations in the cell culture supernatant. We replaced the culture medium and then collected the new one after 90 min (baseline condition); then we replaced it with a new culture medium in the presence of 1 μM norepinephrine for another 90 min. The kit was used according to manufacturer's instructions. Fold change was calculated by the ratio between NE-stimulated glycerol release and the baseline glycerol values within each well.

*RNA extraction, cDNA synthesis, and qPCR*

Total RNA extraction was performed using the NucleoSpinRNA kit (Macherey-Nagel) as specified by the manufacturer. Cells were lyzed in TRIzol (Thermo Fisher) using and mixed with chloroform at 1:5 v/v ratio (chloroform:TRIzol), samples were then centrifuged, and the supernatant transferred into the purification columns of the NucleoSpinRNA kit. All further steps were executed as specified by the manufacturer. cDNA was synthesized with Maxima H Master Mix 5 (Thermo Fisher) using 500 ng of total RNA. Gene expression was evaluated by qPCR using PowerUpSYBR Green Master Mix (Thermo Fisher) according to the manufacturer's instructions. Primers are listed in Supplementary Table 1. Expression was normalized to *Tbp* by the ΔΔct-method.

*Immunoblots*

The samples were lysed in RIPA buffer [50 mM Tris (Merck), pH 8, 150 mM NaCl (Merck), 5 mM EDTA (Merck), 0.1 % w/v SDS (Carl Roth), 1 % w/v IGEPALCA-630 (Sigma), 0.5 % w/v sodium deoxycholate (Sigma)] freshly supplemented with protease inhibitors (Sigma) in a 1:100 v:v ratio and PhosStop phosphatase inhibitors (Roche). Cell lysates were centrifuged for 15 min (4 °C, 12,000 g) and tissue lysates were centrifuged twice for 15 min before the supernatant was collected. Protein concentrations were determined using the Pierce BCA assay (Thermo Fisher) according to the manufacturer's instructions. Protein samples were denatured with 5 % v/v 2-mercaptoethanol (Sigma) for 5 min at 95 °C before they were loaded in Bolt Bis-Tris gels (Thermo Fisher). After separation, proteins were transferred onto a 0.2 mm PVDF membrane (Bio-Rad) using the Trans-Blot Turbosystem (Bio-Rad) at 27 V, 1.4 A for 7 min. The membrane was blocked in Roti-Block (Roth) for 1 h at room temperature. The membranes were incubated overnight in primary antibody dilutions in 5 % w/v BSA-TBS-T at 4 °C. The following primary antibodies were used: ATP5IF1 (Cell Sig. cat. Num. 8528, 1:500), OXPHOS cocktail (Abcam, cat. Num. ab110413, 1:1000), GAPDH (Cell Sig. cat. Num. 5174, 1:2000), total-p38-MAPK (Cell Sig. cat. Num. 9212, 1:2000), p-p38MAPK (Cell Sig. cat. Num. 9211, 1:100), total-AMPK (Cell Sig. cat. Num. 2532, 1:2000), p-AMPK (Cell Sig. cat. Num. 2535, 1:1000), Vinculin (Cell Sig. cat. Num. 4650, 1:5000), and α-tubulin (Sigma, cat. Num. T6074, 1:2000). After washing with TBS-T [200 mM Tris (Merck), 1.36 mM NaCl (Merck), 0.1 % v/v Tween20 (Sigma)], the membranes were incubated in secondary antibody (Santa Cruz) solutions (1:10,000 in Roti-block) for 1 hour at RT. Membranes were washed in TBS-T and imaged using SuperSignal West Pico PLUS (Thermo Fisher) in a Chemidoc imager (Bio-Rad). Images were analyzed using ImageJ (www.imagej.nih.gov).

*Statistical analysis*

Data are shown as individually or mean ± standard deviation (SD). Outliers were removed when the observation was greater than 2 SDs within the same group. Comparisons between two groups were made using a two-tailed Student's t-test while comparisons of three groups were done by using one-way ANOVA followed by LSD post-hoc test. When 2 levels were tested (i.e., treatment vs. IF1 manipulation) 2-way ANOVA followed by LSD post-hoc test was used. Analysis was performed using GraphPad Prism (La Jolla, CA, USA). Statistical difference was considered when $P < 0.05$, indicated by asterisks in the figures.

## Results:

### Cold exposure potentiates the reverse mode of ATP synthase in brown fat

First, we evaluated the hydrolytic activity of ATP synthase, operating in reverse mode in BAT of mice adapted to 4 °C for 5 days. As expected, cold-adapted mice lost body mass despite greater food intake compared to mice kept at room temperature (RT, 22 °C) (Supplementary Fig. 1A, B). We observed that ATP hydrolysis was low in BAT from animals kept at RT. However, cold adaptation was associated with approximately 2-fold higher activity (Fig. 1A, B). In the absence of ATP or $Mg^{2+}$ or in the presence of oligomycin, a classical inhibitor of $F_oF_1$-ATP synthase, ATP hydrolysis was negligible, confirming the assay was specific for measuring the hydrolytic activity of ATP synthase (Fig. 1A). The primary result of ATP hydrolysis by ATP synthase is pumping of protons from the mitochondrial matrix into the intermembrane space. Hence, we tested the contribution of the ATP synthase reverse mode on MMP in isolated mitochondria. For that, we isolated mitochondria from mice kept at RT or adapted to cold and measured MMP using the fluorescent probe safranin-O. Of note, we added antimycin A (to inhibit Complex III) and GDP (to inhibit UCP1) to minimize proton movement through the inner mitochondrial membrane from sources other than ATP synthase activity. Then, we added ATP in the medium to drive ATP synthase into the reverse mode, resulting in ATP hydrolysis and pumping of protons from the mitochondrial matrix into the intermembrane space. As expected, ATP addition caused an increase in MMP in an oligomycin-sensitive manner (Fig. 1C). However, this increase was larger in mitochondria isolated from BAT of cold-exposed mice (Fig. 1D). In summary, this set of data shows that cold adaptation increases the capacity of BAT ATP synthase to function in the reverse mode.

### Cold exposure lowers IF1 levels specifically in brown fat

The small protein IF1 is known to inhibit the hydrolytic activity of ATP synthase in conditions when MMP is low or when the mitochondrial matrix becomes too acidic[15,16]. Therefore, we hypothesized that IF1 was involved in the regulation of ATP synthase function in BAT. When analyzing three different mouse tissues rich in mitochondria (i.e., BAT, liver, and heart), we observed that BAT is characterized by relatively higher levels of IF1 when compared to proteins that compose other mitochondrial respiratory complexes (Fig. 1E, F). Stoichiometrically, this suggests that in BAT, IF1 may exert a profound inhibitory effect on ATP synthase function. Next, we determined mRNA levels of *Atp5if1* in BAT of mice acutely exposed to cold for 4 h or treated with the beta-3 adrenergic agonist CL316,243 and found *Atp5if1* mRNA abundance was approximately 50% lower compared to controls (Fig. 1G). Based on that, we hypothesized low mRNA levels could result in low protein levels once exposure to cold is prolonged. We observed that IF1 protein levels were downregulated by approximately 50 % and 80 % following 3 and 5 days of cold exposure, respectively (Fig. 1H, I). Of note, this cold regimen did not affect IF1 levels in liver and heart (Supplementary Fig. 1C, D), indicating a BAT-specific mechanism. These findings suggest that the reduction of IF1 protein levels after 5 days of cold exposure could explain the greater hydrolytic activity by ATP synthase found in BAT of cold-adapted mice (Fig. 1A-D, J).

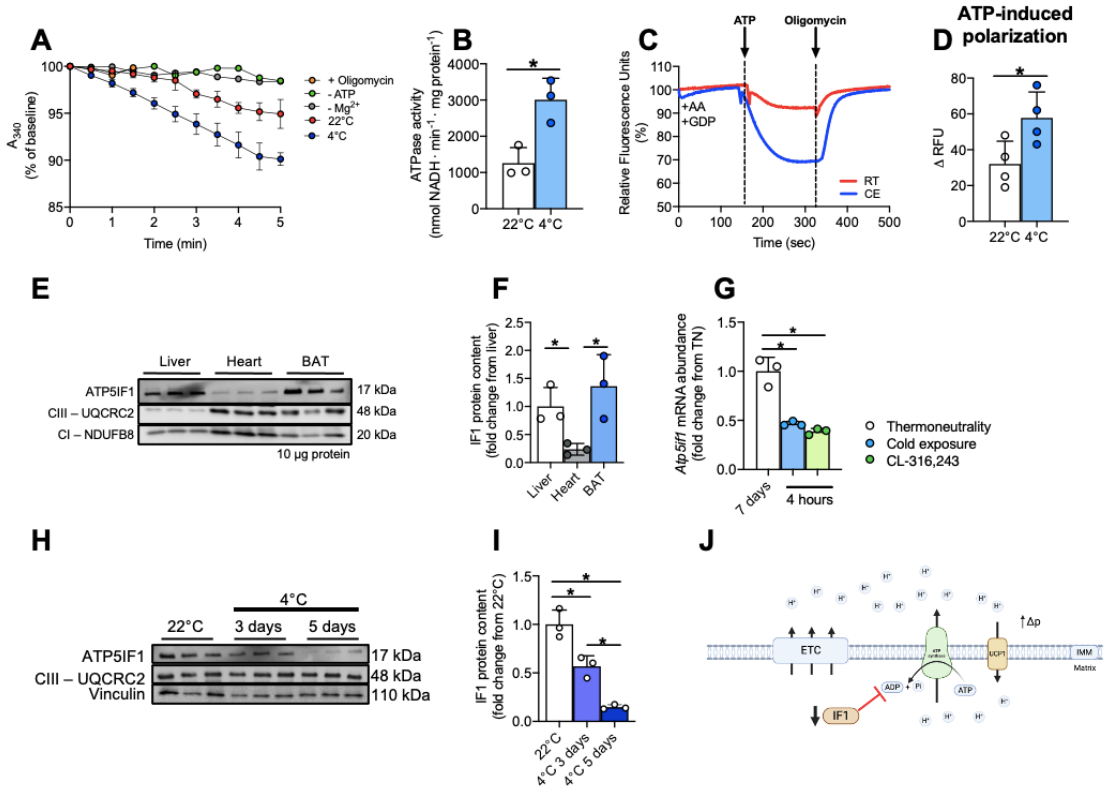


**Fig. 1: Cold favors the reverse mode of ATP synthase and lowers IF1 levels in BAT.**
(A) Representative plots traces of NADH consumption to determine the hydrolytic capacity of ATP synthase and (B) quantification of ATPase activity in BAT from room temperature (RT, 22 °C) or cold-exposed (4 °C) mice. (C) Representative plots of safranin fluorescence in mitochondria isolated from RT or cold-exposed mice in response to ATP addition and (D) quantification of the ATP-induced change in membrane potential. (E) Representative images and (F) quantification of IF1 protein levels in liver, heart, and BAT of mice kept at RT. (G) *Atp5if1* mRNA levels in BAT of thermoneutrality (TN)-adapted mice, 4 hours after cold exposure or CL316,243 injection. (H) Representative images and (I) quantification of IF1 in BAT following 3 or 5 days of cold exposure. (J) Schematic model of the hypothetical relationship between IF1 and UCP1. $A_{340}$: 340 nm absorbance; AA: Antimycin A; RT: room temperature; CE: cold exposure; RFU: relative fluorescence units; ATP5IF1: ATP synthase inhibitory factor subunit-1; BAT: brown adipose tissue; ETC: electron transport chain; IF1: inhibitory factor-1; UCP1: uncoupling protein-1; IMM: inner mitochondrial membrane. Statistical tests: Two-tailed Student's t-test (B, D) and one-way ANOVA followed by LSD post-hoc test (G, I). * $P<0.05$.

## Loss of IF1 does not impact MMP in brown adipocytes

To investigate any causal relationship between the cold-induced downregulation IF1 and MMP due to changes in ATP synthase hydrolytic activity, we first employed an *in vitro* IF1 loss-of-function model, in which we silenced *Atp5if1* mRNA levels using small interfering RNA (siRNA) in cultured differentiated mouse brown adipocytes. We validated our experimental approach by using oligomycin and FCCP, both drugs capable of modulating MMP, to verify the accumulation of TMRM within mitochondria (Supplementary Fig. 2A). As expected, short (i.e., 30 min) pre-treatment with oligomycin increased MMP roughly by 20 % whereas FCCP decreased it by almost 60 %. Interestingly, oligomycin effects over MMP were abrogated once norepinephrine (NE) was added to the media, suggesting the depolarizing effects of UCP1 overcome the increase in MMP induced by oligomycin. Of note, NE has no effects on MMP when FCCP

was present. These data validate that our approach detects changes in MMP. Next, we tested the effects of IF1 silencing on MMP. We started by confirming the efficacy of transfection by observing a ca. 80 % reduction of *Atp5if1* mRNA levels (Fig. 2A) as well as lower protein levels (Fig. 2B) compared to cells treated with non-targeting control siRNA (siScrambled). To mimic cold exposure *in vitro*, we stimulated differentiated adipocytes with 10 μM NE for 30 min before measuring MMP. As expected, NE stimulation increased phosphorylation of p38-MAPK and AMPK, regardless of IF1 levels (Fig. 2C, D), indicating that IF1 did not impact adrenergic signaling. We observed a mild reduction in MMP upon adrenergic stimulation. On the other hand, IF1 ablation did not interfere with the NE-induced reduction in MMP (Fig. 2E). These results demonstrate that loss of IF1 is insufficient to affect MMP in NE-stimulated brown adipocytes.

**High IF1 levels diminish MMP upon adrenergic stimulation**

Next, as IF1 is downregulated with cold, we performed gain-of-function experiments in differentiated brown adipocytes to determine the influence of higher levels of IF1 on MMP upon NE stimulation. Transfection with a vector carrying *Atp5if1* cDNA led to higher IF1 mRNA (Fig. 2F) and protein (Fig. 2G) levels in differentiated mouse brown adipocytes. We confirmed higher p38-MAPK and AMPK phosphorylation levels in NE-stimulated cells compared to non-stimulated (Fig. 2H) and found no effect of IF1 overexpression on adrenergic signaling (Fig. 2I). Upon adrenergic stimulation, however, cells overexpressing IF1 showed a more pronounced drop in MMP (Fig. 2J). These results indicate that IF1 overexpression sensitizes the cells to the ability of NE to decrease MMP. This is consistent with a possible inhibition of the capacity of ATP synthase to operate in the reverse mode, resulting in a lower contribution of ATP synthase to MMP and, consequently, greater depolarization of the mitochondria. Since UCP1 activation is the fundamental event for lowering MMP upon adrenergic stimulation in brown adipocytes, we investigated the necessity of UCP1 for this mechanism to take place. For that, we silenced *Ucp1* mRNA in differentiated brown adipocytes and overexpressed IF1 at the same time (Fig. 2K). While *Ucp1* ablation did not cause any effect on MMP upon adrenergic stimulation, the reduction in MMP observed in cells overexpressing IF1 was abrogated when *Ucp1* was silenced (Fig. 2L). This suggests the proton flux through UCP1 following adrenergic activation is necessary to provide the ideal condition (i.e., low membrane potential) to observe the modulatory effects of IF1 expression on MMP. We next sought to determine whether the effect of IF1 overexpression was specifically related to its binding to ATP synthase. To test this, we overexpressed a mutant IF1 protein harboring an E55A substitution that renders the protein unable to interact with the $F_oF_1$ ATP synthase (Supplementary Fig. 2B). Upon adrenergic stimulation, overexpression of IF1, but not E55A-IF1, reduced MMP in differentiated brown adipocytes (Fig. 2M). In summary, our data show that high levels of IF1 result in mitochondria that cannot sustain MMP upon adrenergic stimulation, and this mechanism is dependent on UCP1.

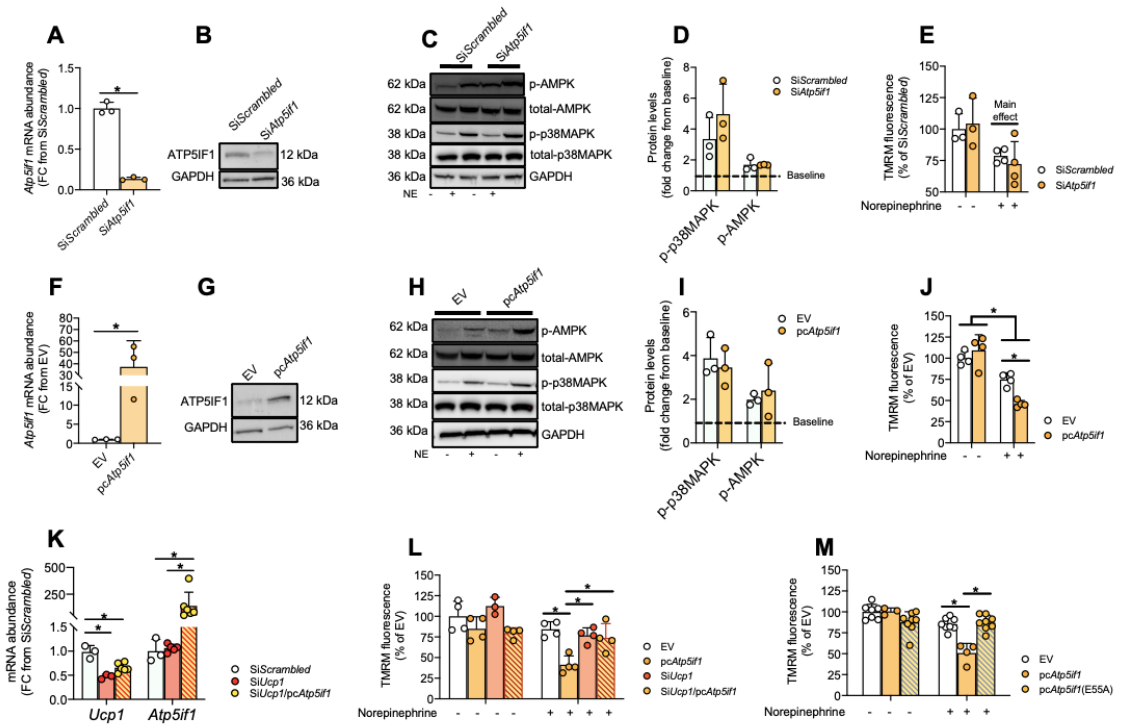


**Fig. 2: IF1 modulates mitochondrial membrane potential upon adrenergic stimulation.** (A,B) *Atp5if1* mRNA and protein levels in differentiated WT1 brown adipocytes. (C,D) Representative western blots and quantification of proteins in norepinephrine (NE)-stimulated (10 μM for 30 minutes) and control WT1 cells, in which *Atp5if1* was knocked down (siAtp5if1) or scramble controls (siScrambled). (E) Relative TMRM fluorescence at baseline and upon NE stimulation in IF1-ablated adipocytes. (F,G) *Atp5if1* mRNA and protein levels following IF1 overexpression in WT1 brown adipocytes. (H,I) Representative western blots and quantification of proteins in NE-stimulated and control WT1 cells, in which IF1 was overexpressed (pcAtp5if1) or empty vector control (EV). (J) Relative TMRM fluorescence at the baseline and following NE stimulation. (K) *Ucp1* and *Atp5if1* mRNA levels following *Ucp1* knockdown or IF overexpression. (L) Relative TMRM fluorescence at baseline and upon NE stimulation in *Ucp1* lacking/IF1 overexpressing WT1 cells. (M) Relative TMRM fluorescence at baseline and following NE stimulation in cells overexpressing mutant IF1(E55A). Atp5if1: ATP synthase inhibitory factor subunit 1; GAPDH: glyceraldehyde-3-phosphate dehydrogenase; TMRM: tetramethylrhodamine methyl ester; FCCP: Carbonyl cyanide-p-trifluoromethoxyphenylhydrazone; p38-MAPK: p38 mitogen-activated protein kinase; NE: norepinephrine; UCP1: uncoupling protein-1; EV: empty vector. Statistical tests: Two-tailed Student's t-test (A, D, F, I), one-way ANOVA followed by LSD post-hoc test (K, M), and two-way ANOVA followed by LSD post-hoc test (E, J, L). * $P<0.05$.

## IF1 silencing increases anaerobic glycolysis to sustain cellular ATP levels

Next, we investigated the metabolic implications of IF1 silencing in primary mouse brown differentiated adipocytes. We confirmed IF1 silencing by observing lower IF1 mRNA (Fig. 3A) and protein (Fig. 3B) levels in the cells upon transfection with siRNA. Then, we determined the oxygen consumption of these cells following NE stimulation. At first, we did not observe any differences in mitochondrial respiration (Fig. 3C, D). It has been suggested that lipolysis caused by adrenergic stimulation could drive mitochondrial uncoupling in a UCP1-independent manner in non-buffered media[26], which could represent a caveat in our experiments. Therefore, we repeated the experiment with the addition of 2 % w/v FFA-BSA to buffer the excess of non-esterified fatty acids released through NE-induced lipolysis. Despite this adjustment of experimental conditions, we did

not detect any effect of IF1 ablation on mitochondrial oxygen consumption (Supplementary Fig. 3A, B). Nevertheless, we detected higher acidification rates in IF1 knockdown cells at baseline and after NE stimulation compared to control cells transfected with scramble siRNA (Fig. 3E, F), suggesting a greater reliance of the cells on anaerobic glycolysis under these conditions. Of note, these differences were not explained by changes in oxidative phosphorylation (OxPhos) subunits (Fig. 3G) or by differences in total cellular ATP levels (Fig. 3H). However, ATP/ADP ratio was lower in IF1-ablated cells compared to scramble controls (Fig. 3I), suggesting that cells with reduced IF1 levels experience mild energetic stress. The reduction in the ATP/ADP ratio is one of the most important determinants of glycolysis [28,29], supporting the notion that an increase in glycolysis could be a compensatory mechanism to sustain ATP levels when IF1 is reduced. To address this possibility, we dissected the contribution of substrates to ATP synthesis using a reductionist, one-substrate approach. For that, we deprived cells of any other exogenous substrate and measured respiration and acidification rates after the injection of glucose. By doing this, we observed that cells lacking IF1 generated more than 75 % of ATP from anaerobic glycolysis and less than 25 % from mitochondrial respiration (Fig. 3J), whereas the source of ATP in control cells was roughly 50 % coming from anaerobic glycolysis and 50 % from mitochondrial respiration.

**IF1 silencing potentiates mitochondrial lipid oxidation in brown adipocytes**

These results prompted us to investigate whether brown fat cells with reduced IF1 levels display altered substrate preference to sustain normal overall respiration. As the measurement of whole-cell oxygen consumption does not differentiate between the substrates being used, we hypothesized that the reduced glucose oxidation in IF1 knockdown cells could be paralleled by greater mitochondrial lipid oxidation, a process using more oxygen to generate ATP in comparison to carbohydrate oxidation. To test this hypothesis, we performed mitochondrial respiration analysis in brown adipocytes in the presence of 100 μM palmitate and in the absence of any other exogenous substrates. Using this experimental design, we observed that adipocytes lacking IF1 displayed higher respiration upon NE stimulation compared to control cells (Fig. 3K, L). To evaluate the extent to which IF1-ablated brown adipocytes depend on lipids to sustain respiration, we measured cellular respiration using cell culture media containing glucose, pyruvate, and glutamine in the presence of etomoxir, an inhibitor of carnitine-palmitoyl transferase 1, the rate-limiting step for lipid utilization within mitochondria. In the presence of etomoxir, mitochondrial respiration as well as NE-driven respiration was roughly 25 % lower in cells with IF1 ablation compared to control cells (Fig. 3M, N). Of note, the metabolic remodeling observed after IF1 ablation resulted in higher lipolytic capacity (Fig. 3O), as observed by greater glycerol release upon adrenergic stimulation. Altogether, these data demonstrate that reducing IF1 levels primes mitochondria to utilize more lipids, thus supporting NE-induced uncoupling and mitochondrial oxygen consumption rate, while a compensatory mechanism increases anaerobic glycolysis to sustain cellular ATP levels.

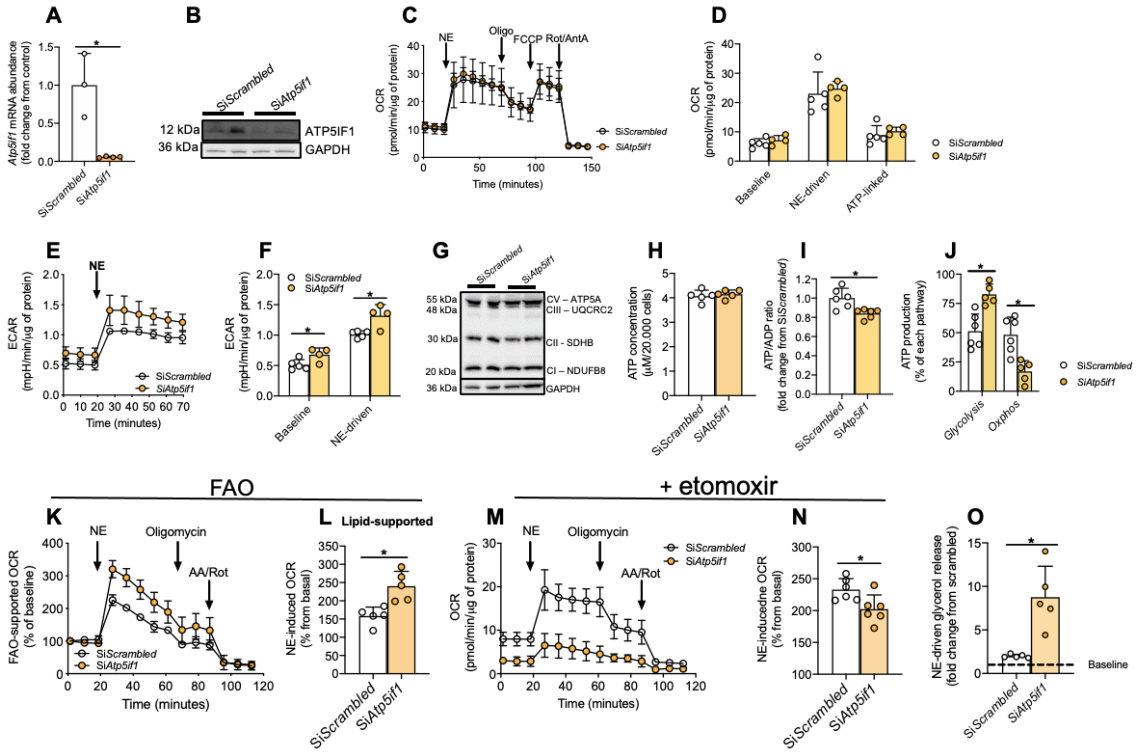


**Fig. 3: IF1 silencing induces mitochondrial lipid oxidation in brown adipocytes.** (A,B) *Atp5if1* mRNA and protein levels. (C,D) Representative plot and quantification of OCR following NE stimulation in primary brown adipocytes upon IF1 knockdown (siAtp5if1) or scramble control (siScrambled). (E,F) Representative plot and quantification of ECR in these cells. (G) Representative western blots of OXPHOS subunits in primary brown adipocytes. (H) Cellular ATP content, (I) ATP/ADP ratio and (J) relative ATP production from glucose. (K) Representative plot of FAO-supported respiration (100 μM palmitate) and (L) quantification of NE-driven OCR. (M) Representative plot and (N) NE-induced respiration in the presence of etomoxir. (O) NE-driven glycerol release. Atp5if1: ATP synthase inhibitory factor subunit-1; GAPDH: glyceraldehyde-3-phosphate dehydrogenase; OCR: oxygen consumption rate; NE: norepinephrine; Oligo: oligomycin; FCCP: carbonyl cyanide-p-trifluoromethoxyphenylhydrazone; Rot: rotenone; AA: antimycin A; ECAR: extracellular acidification rate; FAO: fatty-acid oxidation. Two-tailed Student's t-test (A, D, F, H, I, J, L, N, O). * $P<0.05$.

## IF1 overexpression blunts ATP production in brown adipocytes

As we demonstrated that higher levels of IF1 promote MMP reduction upon NE stimulation, we overexpressed IF1 in differentiated primary mouse brown adipocytes to test the impact of this manipulation on mitochondrial bioenergetics. We first confirmed the overexpression of IF1 upon the transfection protocol by measuring *Atp5if1* mRNA (Fig. 4A) and protein (Fig. 4B) levels. We then measured mitochondrial respiration following acute NE stimulation. We observed a marked reduction in mitochondrial respiration as well as an abrogation of NE-induced uncoupling in cells overexpressing IF1 compared to control cells (Fig. 4C, D). Of note, the addition of 2 % FFA-BSA in the media did not abrogate the inhibitory effects of IF1 overexpression on mitochondrial respiration (Supplementary Fig. 4A, B). Intriguingly, we did not find any compensatory response in anaerobic glycolysis in IF1-overexpressing cells (Fig. 4E, F). Moreover, we observed an almost ca. 50 % reduction in fatty acid-supported mitochondrial respiration at baseline and following NE stimulation in these cells (Fig. 4G, H). Interestingly, overexpression of IF1 impaired mitochondrial respiration despite unchanged protein

content of respiratory complexes (Fig. 4I). The reduction in mitochondrial respiration without any compensatory change in glycolytic activity prompted us to hypothesize that the cells would transition into a quiescence-like state, resulting in overall lower metabolic activity. Therefore, we measured glucose-dependent ATP production from glycolysis and oxidative phosphorylation. We observed that total ATP production was almost ca. 50 % lower in cells overexpressing IF1 (Fig. 4J), and this was explained by lower oxidative phosphorylation-linked ATP production. Correspondingly, cellular ATP content was approximately 50 % lower in IF1 overexpressing cells compared to control cells (Fig. 4K). However, ATP/ADP ratio was not different between the groups (Fig. 4L), suggesting IF1 overexpressing cells do not display energetic stress. Of note, we did not detect any differences in mRNA or protein yield, or in the lipolytic capacity of the cells overexpressing IF1 (Supplementary Fig. 5A-C). Hence, high levels of IF1 blunt mitochondrial respiration, ATP production, and NE-induced uncoupling in brown adipocytes.

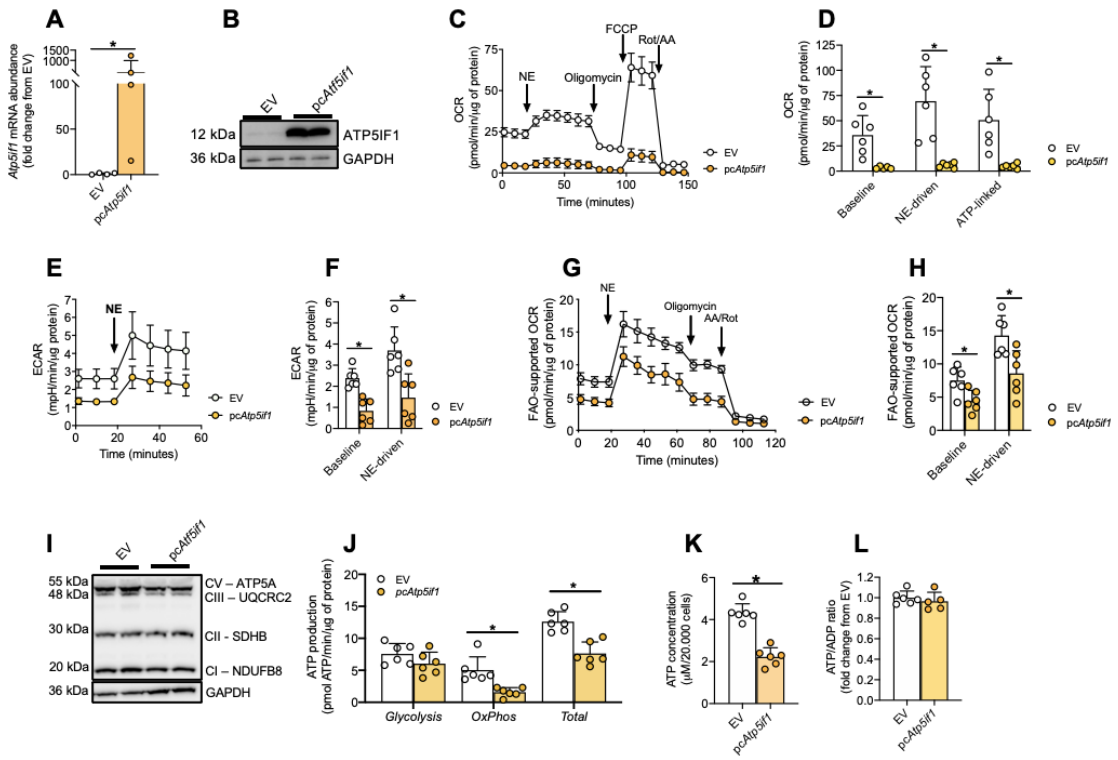


**Fig. 4: IF1 overexpression blunts ATP production in primary brown adipocytes.** (A) *Atp5if1* mRNA and (B) protein levels in primary brown differentiated adipocytes. (C) Representative plot and (D) quantification of oxygen consumption rate following NE stimulation in primary brown adipocytes overexpressing IF1 (pcAtp5if1) or an empty vector (EV). (E) Representative plot and (F) quantification of extracellular acidification rate at baseline and upon NE stimulus. (G) Representative plot of fatty-acid oxidation-supported respiration (100 µM palmitate) and (H) quantification of baseline and NE-driven oxygen consumption. (I) Representative western blots of OXPHOS subunits in primary brown adipocytes. (J) Glycolytic, OxPhos, and total ATP production from glucose; (K) total cell ATP content, and (L) ATP/ADP ratio. Atp5if1: ATP synthase inhibitory factor subunit 1; GAPDH: glyceraldehyde-3-phosphate dehydrogenase; EV: empty vector; OCR: oxygen consumption rate; NE: norepinephrine; Oligo: oligomycin; FCCP: carbonyl cyanide-p-trifluoromethoxyphenylhydrazone; Rot: rotenone; AA: antimycin A; ECAR: extracellular acidification rate; FAO: fatty-acid oxidation. Two-tailed Student's t-test (A, D, F, H, I, J, K, L). * $P<0.05$.

## Discussion

Mitochondria in thermogenic adipocytes experience large fluctuations in metabolic rate and oxygen consumption depending on the ambient temperature and sympathetic activation. Sustaining mitochondrial membrane potential, especially considering the high uncoupling activity of UCP1, is an important aspect of NST. While a lot of work has been focused on the regulation of uncoupled respiration and UCP1, knowledge about coupling regulation remains scarce, especially in brown adipocytes. Here we show that: 1) IF1 is downregulated in cold-adapted BAT, allowing greater hydrolytic activity of ATP synthase by operating in the reverse mode; 2) when IF1 is upregulated in brown adipocytes *in vitro* mitochondria unable to sustain the MMP upon adrenergic stimulation, 3) IF1 ablation in brown adipocytes phenocopies the metabolic adaptation of BAT to cold, and 4) IF1 overexpression blunts mitochondrial respiration without any apparent compensatory response in glycolytic activity. Hence, our data provide an explanation for the reduction of IF1 levels in BAT during cold exposure, as this would represent a necessary mechanism to allow proper adaptation of energy metabolism during NST with high of UCP1 activity and uncoupling.

The tight relationship between activity of the electron transport chain and oxygen consumption has long been recognized since the work by Chance and Williams[30]. Later, Peter Mitchell proposed that the electrochemical gradient generated by the electron transport chain is coupled to ATP synthesis, driven by proton motive force[11]. Therefore, respiration rate is controlled in a non-linear fashion directly by the MMP, which depends on ATP synthase activity and energy demand. This elegant model is challenged in brown adipocytes by the unique presence of UCP1, which is activated upon adrenergic signaling, allowing proton flux from the intermembrane space into the mitochondrial matrix[1,8]. Although this system allows animals to adapt to cold environments, sustained and uncontrolled lowering of MMP due to protons constantly entering the mitochondrial matrix may represent a threat to mitochondrial function and cellular homeostasis. For example, collapse of the MMP results in cytochrome c release and mitochondrial-induced apoptosis. Therefore, mitochondria bear mechanisms to fine-tune MMP[18], as in BAT of cold-adapted rats, the capacity of ATP synthesis in mitochondria is preserved, whereas ATP hydrolysis is increased by almost 6-fold[31]. At that time, Yamada et al. proposed the existence of an unknown mechanism capable of controlling the counterclockwise rotation (hydrolysis) of $F_oF_1$-ATP synthase without affecting its clockwise activity (synthesis)[31]. Now, our results provide a mechanism underlying the low capacity of BAT mitochondria to synthesize ATP. Also, it has been hypothesized that this phenomenon is caused by the relatively low expression of complex V[32]. However, considering that IF1 inhibits $F_1$-ATP synthase in a 1:1 stoichiometric ratio, the relatively higher expression of IF1 in BAT at room temperature could represent an additional inhibitory factor for ATP synthesis in this tissue.

Agreeing with the prediction by Yamada et al. and providing a mechanistic explanation for the phenomenon, our data reveal that IF1 is downregulated in BAT following cold exposure, thus facilitating the hydrolytic activity of ATP synthase and, possibly, sustaining MMP. The suppressive effects of IF1 on MMP is blunted once a mutated IF1 incapable of binding to ATP synthase, is introduced, further demonstrating the effects of IF1 are mediated by the binding of IF1 to ATP synthase. Importantly, this mechanism is dependent on UCP1, as UCP1 activation is necessary for the effects of IF1 manipulation

on MMP in brown adipocytes. Hence, it is unsurprising that this mechanism is specifically observed in BAT and manifests upon cold/adrenergic stimulation. Indeed, in both gain- and loss-of-function experiments, we did not observe effects of IF1 manipulation on MMP at baseline conditions. However, IF1 appears to be important to control MMP in brown adipocytes upon adrenergic stimulation, when UCP1 activation allows increased proton movement into the mitochondrial matrix. Therefore, it is plausible to speculate that the reduction of MMP upon adrenergic stimulation in IF1 overexpressing brown adipocytes is a result of an inability of the ATP synthase to pump protons back into the intermembrane space, caused by the inhibition of its hydrolytic activity, independent of the involvement of ATP synthase activity. An alternative hypothesis is that IF1 overexpression elicits changes in electron transport chain activity that do not match the activity of UCP1, resulting in a collapse of MMP upon adrenergic stimulation.

Beyond changes in MMP, alterations in IF1 levels exert profound metabolic effects on brown adipocytes. Activation of BAT is associated with an increase in energy expenditure in the tissue as well as at the whole-body level. At the tissue level, BAT activation increases both lipid and glucose uptake[6,33,34]. Since glucose can be converted into lactate in the cytosol, it is believed that lipids are the main energy-equivalent providers to the mitochondria to support respiration during BAT activation. This theoretical argument is supported by a marked reduction in respiratory exchange ratio upon adrenergic beta-3 agonist activation[7]. Interestingly, lowering IF1 levels is sufficient to prime brown adipocytes *in vitro* toward lipid utilization. Given that β-oxidation produces a higher $FADH_2$/NADH ratio compared to glucose oxidation, fatty acid oxidation has a more pronounced effect on the increase in oxygen consumption (FAD-supported P/O ratio = 1.5; NAD-supported P/O ratio = 2.5) than glucose. In support of greater mitochondrial lipid utilization, we observed the contribution of glycolysis to ATP production was increased in cells with reduced IF1 levels, possibly facilitated by a lower ATP/ADP ratio. These data show that brown adipocytes with low IF1 levels rely more on glycolysis as an energy source while lipids feed the TCA cycle to support uncoupled mitochondrial respiration.

In BAT, we observed significant amounts of IF1 when animals are kept at room temperature, which for mice is already a relatively cold environment. Despite the downregulation by further cold exposure, it is intriguing why BAT would still express IF1, especially considering the relatively low expression of mitochondrial complex V. IF1 overexpression *in vitro* markedly suppressed mitochondrial respiration in differentiated brown adipocytes, despite no changes in MMP under unstimulated conditions. This suggests that IF1 may also control metabolism independently of its role in regulating MMP. A dual function of IF1 (inhibitor of ATP hydrolysis and synthesis) has been recently proposed by several groups[35–37]. Our data support these findings, as we observed a profound reduction in mitochondrial respiration regardless of the substrate offered. Interestingly, we found that the cells responded normally to adrenergic stimulation as well as to all inhibitors/uncouplers used in the respiration protocol, although at lower magnitude compared to control cells. This suggests that IF1 controls not only ATP synthase activity but also electron transport chain activity.

The levels of OxPhos complexes are unchanged in cells overexpressing IF1, excluding the possibility that low respiration could be a result of diminished mitochondrial content in brown adipocytes. Thus, IF1 overexpression does not appear to induce an overall mitochondrial dysfunction, but rather an apparent quiescent-like state in the cells, perhaps similar to what is observed in mice at thermoneutrality. This hypothesis is supported by the absence of metabolic compensatory mechanisms otherwise commonly found in models of mitochondrial dysfunction, such as increases in glycolysis, glycolysis-supported ATP production, or ATP/ADP ratio[37,38]. It is noteworthy that upon cold adaptation, BAT undergoes massive remodeling as observed by cell proliferation, inhibition of apoptosis, protein and lipid synthesis, and tissue expansion[38]. It has been recently demonstrated that chronic inhibition of ATP synthase in dividing fibroblasts modulates metabolic rate due to epigenetic modifications, suggesting retrograde signaling from mitochondria to nuclei to control metabolic rate[39]. This retrograde signaling is also observed in other contexts (i.e., cancer cells, skeletal muscle, or cardiomyocytes) where IF1 manipulation profoundly affects cellular metabolism and adaptation to stress[18,36,37,40]. Thus, we speculated that higher levels of IF1 in BAT support brown fat cells remaining in a quiescent-like state when NST is not fully activated. In contrast, once BAT activity is induced upon adrenergic stimulation and metabolic remodeling is necessary, IF1 is reduced allowing an enhanced NST response by the cells.

It remains unclear how IF1 is downregulated following cold exposure. Notably, a few hours of cold exposure or CL administration in mice decreased *Atp5if1* mRNA levels in BAT by almost 50%, suggesting that the downregulation of IF1 may be controlled acutely at the transcriptional level. It has also been shown that immediate early response 1 (IEX1) targets IF1 for degradation[41]. While IEX1 KO mice are protected from high-fat diet-induced insulin resistance through browning of adipose tissue, the response of IEX1 to cold exposure in BAT is unknown[42]. Therefore, proteolytic control of IF1 following cold exposure cannot be ruled out. Of note, proteomic analysis of adult human BAT shows an increase of IF1 content following 4 and 24 hours of cold exposure[43], which suggest that the time course of IF1 regulation may be different between mice and humans. In conclusion, we introduce the concept that by regulating IF1 levels, brown adipocytes are adapting mitochondrial and cellular metabolism to support NST. Given the importance of IF1 to control brown adipocyte energy metabolism, lowering IF1 levels therapeutically might enhance approaches to enhance NST for improving cardiometabolic health in humans.

**Acknowledgment**
We thank Elzira Saviani, Silvia Weidner, and Thomas Pitsch for their excellent technical assistance. We thank the members of Bartelt Lab for enjoyable atmosphere and stimulating discussions. H.S.B. was supported by the Fundação de Amparo à Pesquisa do Estado de São Paulo – FAPESP (2019/21852-1, 2022/00358-1, 2021/08354-2). A.B. was supported by the Deutsche Forschungsgemeinschaft (SFB1123-B10 & SPP2306 BA4925/2-1), the Deutsches Zentrum für Herz-Kreislauf-Forschung DZHK, and the ERC Starting Grant PROTEOFIT. We apologize to colleagues whose work we could not cite due to space limitations. The graphical abstract was created using BioRender.com.

**Competing interest**
The authors declare no competing financial interests related to this work.

**Author contributions**

H.S.B. designed and performed experiments, analyzed data, and wrote the manuscript. A.S.J. and A.F. designed and performed experiments. R. F. C. and M.A.M. designed experiments, analyzed data, and edited the manuscript. A.B. designed experiments, analyzed data, and wrote the manuscript. All authors read and commented on the manuscript.

**References**
1. Cannon, B. & Nedergaard, J. Brown Adipose Tissue: Function and Physiological Significance. *Physiol. Rev.* **84**, 277–359 (2004).
2. Nicholls, D. G. Mitochondrial proton leaks and uncoupling proteins. *Biochim. Biophys. Acta - Bioenerg.* **1862**, 148428 (2021).
3. Fedorenko, A., Lishko, P. & Kirichok, Y. Mechanism of fatty-acid-dependent UCP1 uncoupling in brown fat mitochondria. *Cell* **151**, 400–413 (2012).
4. Brunetta, H. S. *et al.* Nitrate attenuates high fat diet-induced glucose intolerance in association with reduced epididymal adipose tissue inflammation and mitochondrial reactive oxygen species emission. *J of Physiol* vol. **598** (2020).
5. Fromme, T. *et al.* Degradation of brown adipocyte purine nucleotides regulates uncoupling protein 1 activity. *Mol. Metab.* **8**, 77–85 (2018).
6. Bartelt, A. *et al.* Brown adipose tissue activity controls triglyceride clearance. *Nat. Med.* **17**, 200–206 (2011).
7. Politis-Barber, V. *et al.* Ckmt1 is Dispensable for Mitochondrial Bioenergetics Within White/Beige Adipose Tissue. *Function* **3**, 1–16 (2022).
8. Matthias, A., Jacobsson, A., Cannon, B. & Nedergaard, J. The bioenergetics of brown fat mitochondria from UCP1-ablated mice. UCP1 is not involved in fatty acid-induced de-energization ('uncoupling'). *J. Biol. Chem.* **274**, 28150–28160 (1999).
9. Chouchani, E. T., Kazak, L. & Spiegelman, B. M. New Advances in Adaptive Thermogenesis: UCP1 and Beyond. *Cell Metab.* **29**, 27–37 (2019).
10. Nicholls, D. G. Fifty years on: How we uncovered the unique bioenergetics of brown adipose tissue. *Acta Physiol.* **237**, (2023).
11. Mitchell, P. Coupling of phosphorylation to electron and hydrogen transfer by a chemi-osmotic type of mechanism. *Nature* **191**, 144–148 (1961).
12. Kobayashi, R., Ueno, H., Okazaki, K. I. & Noji, H. Molecular mechanism on forcible ejection of ATPase inhibitory factor 1 from mitochondrial ATP synthase. *Nat. Commun.* **14**, 1682 (2023).
13. Gledhill, J. R., Montgomery, M. G., Leslie, A. G. W. & Walker, J. E. How the

regulatory protein, IF1, inhibits F1-ATPase from bovine mitochondria. *Proc. Natl. Acad. Sci. U. S. A.* **104**, 15671–15676 (2007).
14. Cabezón, E., Montgomery, M. G., Leslie, A. G. W. & Walker, J. E. The structure of bovine F 1 -ATPase in complex with its regulatory protein IF 1. *Nat. Struct. Biol.* **10**, 744–750 (2003).
15. Pullman, M. E. & Monroy, G. C. a Naturally Occurring Inhibitor of Mitochondrial Adenosine. *J. Biol. Chem.* **238**, 3762–3769 (1963).
16. Esparza, P. B., Cristina, M., Tapioles, N. & Cuezva, J. M. Regulation of the -$H^+$-ATP synthase by IF1: a role in mitohormesis. *Cell Mol. Life Sci.* **74**, 2151–2166 (2017).
17. Nelson, M. A. M. *et al.* Intrinsic OXPHOS limitations underlie cellular bioenergetics in leukemia. *Elife* 1–31 (2021).
18. Chen, W. W. *et al.* Report Inhibition of ATPIF1 Ameliorates Severe Mitochondrial Respiratory Chain Dysfunction in Mammalian Cells. *Cell Rep.* 27–34 (2014) doi:10.1016/j.celrep.2014.02.046.
19. Acin-perez, R. *et al.* Inhibition of ATP synthase reverse activity restores energy homeostasis in mitochondrial pathologies. *EMBO J.* 1–21 (2023) doi:10.15252/embj.2022111699.
20. Petrick, H. L. *et al.* Dietary nitrate increases submaximal SERCA activity and ADP transfer to mitochondria in slow-twitch muscle of female mice. *Am. J. Physiol. - Endocrinol. Metab.* **323**, E171–E184 (2022).
21. Brunetta, H. S. *et al.* Nitrate consumption preserves HFD-induced skeletal muscle mitochondrial ADP sensitivity and lysine acetylation: A potential role for SIRT1. *Redox Biol.* **52**, (2022).
22. Francisco, A., Ronchi, J. A., Navarro, C. D. C., Figueira, T. R. & Castilho, R. F. Nicotinamide nucleotide transhydrogenase is required for brain mitochondrial redox balance under hampered energy substrate metabolism and high-fat diet. *J. Neurochem.* **147**, 663–677 (2018).
23. Petrick, H. L. *et al.* In vitro ketone-supported mitochondrial respiration is minimal when other substrates are readily available in cardiac and skeletal muscle. *J. Physiol.* **598**, 4869–4885 (2020).
24. Willemsen, N., Arigoni, I., Studencka-Turski, M., Krüger, E. & Bartelt, A. Proteasome dysfunction disrupts adipogenesis and induces inflammation via ATF3. *Mol. Metab.* **62**, 101518 (2022).
25. Ruas, J. S., Siqueira-Santos, E. S., Rodrigues-Silva, E. & Castilho, R. F. High glycolytic activity of tumor cells leads to underestimation of electron transport system capacity when mitochondrial ATP synthase is inhibited. *Sci. Rep.* **8**, 1–17 (2018).
26. Li, Y., Fromme, T., Schweizer, S., Schöttl, T. & Klingenspor, M. Taking control over intracellular fatty acid levels is essential for the analysis of thermogenic function in cultured primary brown and brite/beige adipocytes. *EMBO Rep.* **15**, 1069–1076 (2014).
27. Mookerjee, S. A., Gerencser, A. A., Nicholls, D. G. & Brand, M. D. Quantifying intracellular rates of glycolytic and oxidative ATP production and consumption using extracellular flux measurements. *J. Biol. Chem.* **292**, 7189–7207 (2017).
28. Kemp, R. G. & Gunasekera, D. Evolution of the allosteric ligand sites of mammalian phosphofructo-1-kinase. *Biochemistry* **41**, 9426–9430 (2002).
29. Schormann, N., Hayden, K. L., Lee, P., Banerjee, S. & Chattopadhyay, D. An overview of structure, function, and regulation of pyruvate kinases. *Protein Sci.* **28**, 1771–1784 (2019).
30. Chance, B. & Williams, G. Respiratory enzymes in the oxidative phosphorylation. *Nature* (1955).
31. Yamada, E. W., Huzel, N. J., Bosf, R., Kates, A. & Himms-hagen, J. ATPase-inhibitor proteins of brown-adipose-tissue mitochondria from warm- and cold-acclimated rats. *Biochem. J.* **287**, 151–157 (1992).

32. Cannon, B. & Vogel, G. The mitochondrial ATPase of brown adipose tissue Purification and comparison with the mitochondrial ATPase from beef heart. *FEBS Lett.* **76**, 284–289 (1977).
33. Sponton, C. H., de Lima-Junior, J. C. & Leiria, L. O. What puts the heat on thermogenic fat: metabolism of fuel substrates. *Trends Endocrinol. Metab.* **33**, 587–599 (2022).
34. Hankir, M. K. & Klingenspor, M. Brown adipocyte glucose metabolism: a heated subject. *EMBO Rep.* **19**, 1–13 (2018).
35. Formentini, L. *et al.* Mitochondrial H+-ATP synthase in human skeletal muscle: contribution to dyslipidaemia and insulin resistance. *Diabetologia* **60**, 2052–2065 (2017).
36. Sánchez-González, C. *et al.* Dysfunctional oxidative phosphorylation shunts branched-chain amino acid catabolism onto lipogenesis in skeletal muscle. *EMBO J.* **39**, (2020).
37. Zhou, B. *et al.* Upregulation of mitochondrial ATPase inhibitory factor 1 (ATPIF1) mediates increased glycolysis in mouse hearts. *J. Clin. Invest.* **132**, (2022).
38. Nedergaard, J., Wang, Y. & Cannon, B. Cell proliferation and apoptosis inhibition: essential processes for recruitment of the full thermogenic capacity of brown adipose tissue. *Biochim. Biophys. Acta - Mol. Cell Biol. Lipids* **1864**, 51–58 (2019).
39. Sturm, G. *et al.* OxPhos defects cause hypermetabolism and reduce lifespan in cells and in patients with mitochondrial diseases. *Commun. Biol.* **6**, 1–22 (2023).
40. Formentini, L. *et al.* The Mitochondrial ATPase Inhibitory Factor 1 Triggers a ROS-Mediated Retrograde Prosurvival and Proliferative Response. *Mol. Cell* **1**, 731–742 (2012).
41. Shen, L., Zhi, L., Hu, W. & Wu, M. X. IEX-1 targets mitochondrial F1Fo-ATPase inhibitor for degradation. *Cell Death Differ.* **16**, 603–612 (2009).
42. Shahid, M. *et al.* IEX-1 deficiency induces browning of white adipose tissue and resists diet-induced obesity. *Sci. Rep.* 1–14 (2016) doi:10.1038/srep24135.
43. Forner, F. *et al.* Proteome Differences between Brown and White Fat Mitochondria Reveal Specialized Metabolic Functions. *Cell Metab.* **10**, 324–335 (2009).

## Supplementary Figures & Table

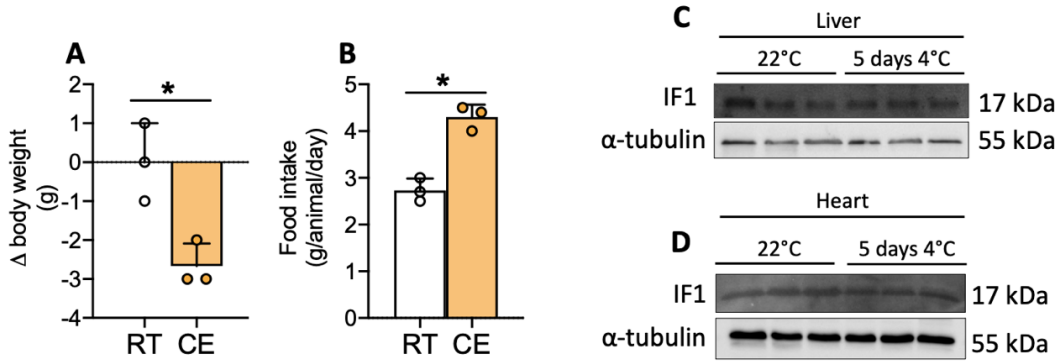


**Supplementary Fig. 1: Cold exposure lowers body weight and does not alter IF1 levels in liver and heart.** (A) Variation of body weight and (B) food intake during 5 days of cold exposure. IF1 protein levels in (C) liver and (D) heart after 5 days of cold exposure. IF1: ATP synthase inhibitory factor subunit-1; Two-tailed Student's t-test (A, B). * *P*<0.05.

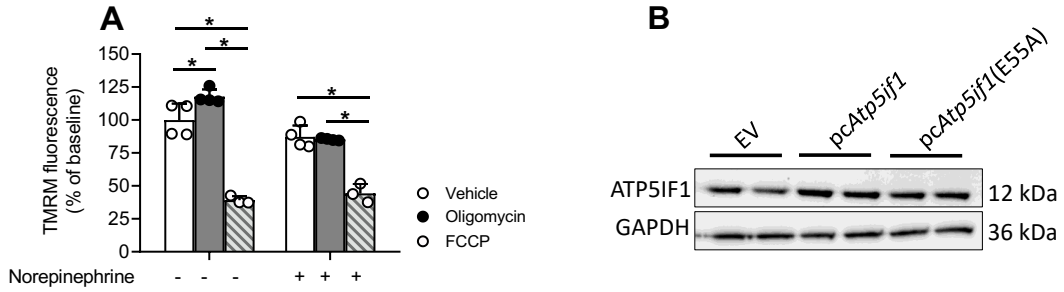


**Supplementary Fig. 2: Effects of oligomycin and FCCP on mitochondrial membrane potential.** Brown adipocytes were pre-treated (30 min) with FCCP or oligomycin before the addition of norepinephrine. Norepinephrine treatment lasted 30 minutes before the cells were loaded with 20 nM TMRM. B) Representative blot of IF1 mutant overexpression in differentiated WT1 brown adipocytes. FCCP: Carbonyl cyanide-p-trifluoromethoxyphenylhydrazone; TMRM: tetramethylrhodamine methyl ester. Statistical test: one-way ANOVA followed by LSD post-hoc test. **P*<0.05.

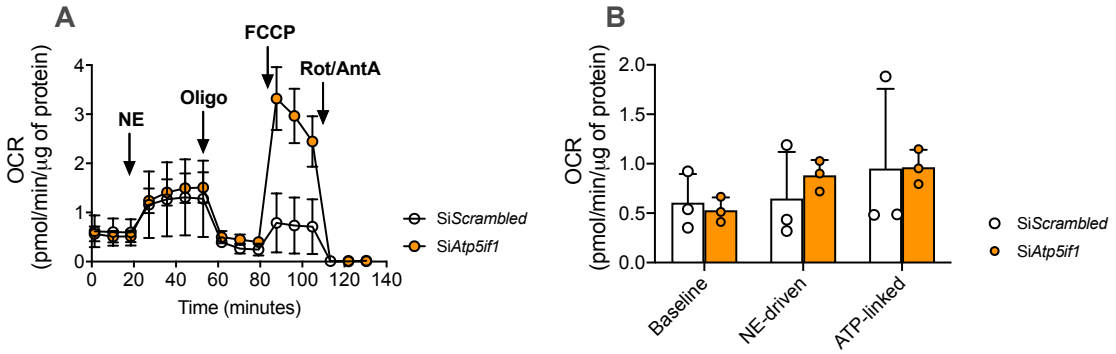


**Supplementary Fig. 3: Presence of FFA-BSA does not alter mitochondrial respiration in IF1 knockdown adipocytes.** (A) Representative trace and (B) quantification of mitochondrial oxygen consumption rate in primary brown adipocytes knockdown for IF1 (siAtp5if1) or controls (siScrambled). Atp5if1: ATP synthase inhibitory factor subunit 1; OCR: oxygen consumption rate; NE: norepinephrine; Oligo: oligomycin; FCCP: carbonyl cyanide-p-trifluoromethoxy-phenylhydrazone; Rot: rotenone; AA: antimycin A. Two-tailed Student's t-test. **P*<0.05.

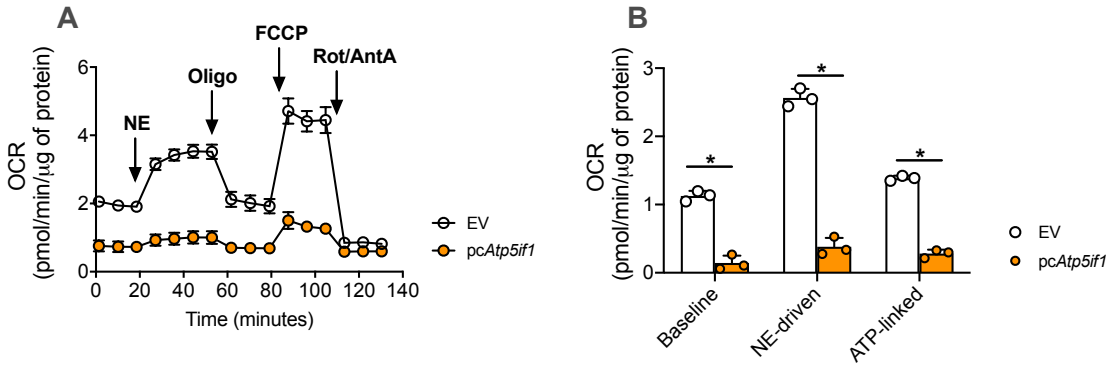


**Supplementary Fig. 4: Presence of FFA-BSA does not alter mitochondrial respiration in IF1-overexpressing adipocytes.** (A) Representative trace and (B) quantification of mitochondrial oxygen consumption rate in primary brown adipocytes overexpressing IF1 (pcAtp5if1) or controls (EV). Atp5if1: ATP synthase inhibitory factor subunit 1; OCR: oxygen consumption rate; NE: norepinephrine; Oligo: oligomycin; FCCP: carbonyl cyanide-p-trifluoromethoxyphenylhydrazone; Rot: rotenone; AA: antimycin A. Two-tailed Student's t-test. *$P$<0.05.

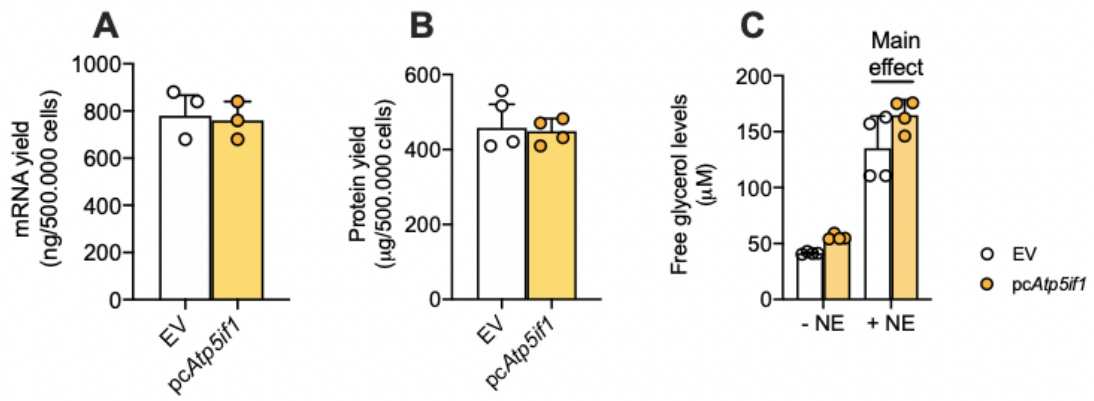


**Supplementary Fig. 5: IF1 overexpression does not affect basic cell parameters in brown adipocytes.** (A,B) mRNA and protein yield from 500.000 cells overexpressing IF1. (C) Norepinephrine-induced lipolysis in IF1 overexpressing adipocytes. Atp5if1 - ATP synthase inhibitory factor subunit 1; NE – norepinephrine. Two-tailed Student's t-test. * p<0.05.

**Supplementary Table 1 – primer sequences.**

| Gene | Forward sequence | Reverse sequence |
|---|---|---|
| *Tbp* | AGA ACAATCCAGACTAGCAGCA | GGGAACTTCACATCACAGCTC |
| *Atp5if1* | GGTTCGGTGTCTGGGGTATG | ATCCATGCTATCCGACGAGT |
| *Ucp1* | AGGCTTCCAGTACCATTAGGT | CTGAGTGAGGCAAAGCTGATTT |